



ANIMAL MODELS

Impact of Prostate Inflammation on Lesion Development in the POET3⁺ *Pten*^{+/-} Mouse Model of Prostate Carcinogenesis

Grant N. Burcham,^{*†} Gregory M. Cresswell,^{*} Paul W. Snyder,^{*‡} Long Chen,[§] Xiaoqi Liu,^{§‡} Scott A. Crist,^{*‡} Michael D. Henry,[¶] and Timothy L. Ratliff^{*‡}

From the Department of Comparative Pathobiology,^{*} College of Veterinary Medicine, and the Department of Biochemistry,[§] College of Agriculture, Purdue University, West Lafayette, Indiana; the Heeke Animal Disease Diagnostic Laboratory,[†] Southern Indiana Purdue Agricultural Center, Dubois, Indiana; the Purdue University Center for Cancer Research,[‡] West Lafayette, Indiana; and the Department of Physiology and Biophysics and Holden Comprehensive Cancer Center,[¶] Roy J. and Lucille A. Carver College of Medicine, University of Iowa, Iowa City, Iowa

Accepted for publication
August 20, 2014.

Address correspondence to
Timothy L. Ratliff, Ph.D.,
Purdue University Center for
Cancer Research, Hansen Life
Sciences Research Bldg., 201 S.
University St., West Lafayette,
IN 47907-2064. E-mail:
tratliff@purdue.edu.

Evidence linking prostatitis and prostate cancer development is contradictory. To study this link, the POET3 mouse, an inducible model of prostatitis, was crossed with a *Pten*-loss model of prostate cancer (*Pten*^{+/-}) containing the ROSA26 luciferase allele to monitor prostate size. Prostatitis was induced, and prostate bioluminescence was tracked over 12 months, with lesion development, inflammation, and cytokine expression analyzed at 4, 8, and 12 months and compared with mice without induction of prostatitis. Acute prostatitis led to more proliferative epithelium and enhanced bioluminescence. However, 4 months after initiation of prostatitis, mice with induced inflammation had lower grade preneoplastic lesions. A trend existed toward greater development of carcinoma 12 months after induction of inflammation, including one of two mice with carcinoma developing perineural invasion. Two of 18 mice at the later time points developed lesions with similarities to proliferative inflammatory atrophy, including one mouse with associated carcinoma. *Pten*^{+/-} mice developed spontaneous inflammation, and prostatitis was similar among groups of mice at 8 and 12 months. Analyzed as one cohort, lesion number and grade were positively correlated with prostatitis. Specifically, amounts of CD11b⁺Gr1⁺ cells were correlated with lesion development. These results support the hypothesis that myeloid-based inflammation is associated with lesion development in the murine prostate, and previous bouts of CD8-driven prostatitis may promote invasion in the *Pten*^{+/-} model of cancer. (*Am J Pathol* 2014, 184: 3176–3191; <http://dx.doi.org/10.1016/j.ajpath.2014.08.021>)

The importance of the immune system and chronic inflammation in the pathogenesis of cancer development has been recognized by recent inclusion of inflammation as an enabling characteristic of cancer formation.¹ Inflammation has been shown to promote tumor formation in multiple tissues, with some of the most notable examples in the gastrointestinal tract, including reflux esophagitis and esophageal cancer, *Helicobacter*-associated gastritis and gastric cancer, and inflammatory bowel disease and colorectal cancer.^{2–4}

Both prostate cancer and prostatitis are common diseases in American men; prostate cancer is the most common malignancy in American men, and the prevalence of prostatitis is as high as 9% by age 79 years according to one Minnesota-based study.⁵ Given the high prevalence of both diseases and the

association between chronic inflammation and cancer, a causal relation between the two diseases seems plausible. However, current epidemiologic and clinical evidence about the relation between inflammation and carcinogenesis in the prostate is contradictory.

Within the past year, a meta-analysis including 20 relatively recent case-control and cohort studies examining the link between prostatitis and prostate cancer found a positive

Supported by NIH grants R01 DK84454 (T.L.R.), R21 CA154126 (M.D.H. and T.L.R.), and 5T32OD011122 (salary support for G.N.B.) and Purdue University Center for Cancer Research grant P30 CA023168 (T.L.R.).

Disclosures: None declared.

association between the presence of inflammation and prostate cancer development.⁶ In addition in 2013, a study of prostatitis and benign prostatic hyperplasia found a relevant association between prostatitis and prostate cancer and between benign prostatic hyperplasia and cancer development in Asian men, a population with lower overall incidence of prostate cancer.⁷ Concurrently, two biopsy-based studies were published that identified and scored both acute and chronic inflammation in prostatic biopsies that were negative for carcinoma on initial screening. Both studies, one performed in Finland, the other in the United States, found that the presence of acute or chronic inflammation on the initial biopsy was negatively associated with development of prostate cancer in follow-up biopsies.^{8,9} Interestingly, in both studies the presence of acute prostatitis on the initial screening resulted in a lower cumulative risk for development of prostate cancer in subsequent screenings.

Many epidemiologic studies about anti-inflammatory treatment and prostate cancer risk have also been conducted, with similarly conflicting results. In several studies, taking aspirin is associated with decreased prostate cancer risk, whereas other nonsteroidal anti-inflammatories either increase prostate cancer risk or have no effect.^{10,11} Other studies show that aspirin treatment has no protective effect on prostate cancer development, and other nonsteroidal anti-inflammatories have only a modest effect.¹² History of sexually transmitted disease has also been variably associated with prostate cancer development. In results from a recent prospective study of men's health in California, the presence of prostatitis was positively associated with prostate cancer development, but previous infection with a sexually transmitted disease increased the risk of prostate cancer development only in certain ethnic groups, a finding at odds with previous studies of sexually transmitted diseases and prostate cancer risk.¹³ Taken together, the published epidemiologic and clinical data linking prostatitis and cancer development are mixed, with strong recent evidence to suggest that the presence of histologically confirmed prostatitis is protective for prostate cancer development.

Other approaches have also been used to examine this potential link, including *in vitro* studies using prostate cancer cell lines and treatment with inflammatory cytokines and *in vivo* studies using animal models. As one example of the *in vitro* evidence linking prostatitis and cancer development, studies examining the effects of IL-6 on prostate cancer cell line growth confer a growth advantage and enhanced vascular endothelial growth factor production to chronically treated LNCaP cells.^{14,15} Animal models of prostatitis have been developed, with a few used to investigate inflammation's effect on carcinogenesis *in vivo*. With the use of uropathogenic *Escherichia coli* infection of the prostate as a model of prostate inflammation, previously infected murine prostates showed enhanced hyperplasia and dysplasia with higher degrees of oxidative damage to epithelial cell DNA, suggesting inflammation can lead to the early steps of cellular

transformation.¹⁶ In another mouse model, inhibitor of NF- κ B (I κ B) kinase 2 was constitutively activated in the prostate of mice with prostate-specific deletion of the tumor suppressor *Pten*. I κ B kinase 2 activation mimics chronic inflammation through downstream activation of NF- κ B, a master transcription factor for several proinflammatory pathways. Here, mice with both activation of I κ B kinase 2 and loss of one allele of *Pten* had larger epithelial lesions and increased fibrous stroma in the prostate compared with mice with loss of *Pten* only but no development of invasive lesions.¹⁷ Thus, pieces of *in vitro* and *in vivo* evidence suggest a positive association between inflammation and prostate carcinogenesis.

We are interested in investigating the effects of prostatitis on prostate cancer development in an animal model relevant to both diseases. Prostatitis is currently classified as acute bacterial, chronic bacterial, asymptomatic inflammatory, or chronic prostatitis/chronic pelvic pain syndrome (CP/CPPS), which can be either inflammatory or noninflammatory.¹⁸ Approximately 90% of all cases of prostatitis are diagnosed as CP/CPPS, which has evidence for an autoimmune component as part of the syndrome's complex pathogenesis.¹⁹ Because many cases of prostatitis may have an autoimmune component, the POET-3 mouse model of prostatitis was developed and previously characterized by our laboratory.²⁰ This model makes use of the availability of tools already in place by using ovalbumin as a prostate-specific model antigen. Prostatitis is induced in a controlled manner via adoptive transfer of preactivated CD8⁺ OT-I T cells, which bear a transgenic T-cell receptor recognizing a peptide in the ovalbumin protein. Acute prostatitis is followed by a chronic phase, with detection of enhanced concentrations of leukocytes up to 80 days after induction of inflammation.²⁰ This model was crossed with the C57/Luc/*Pten*^{+/-} mouse model of prostate carcinogenesis, which uses the Cre-loxP system driven by the prostate-specific Probasin promoter to inactivate one allele of *Pten* in the prostate.²¹ The prostate-specific expression of luciferase allows for *in vivo* imaging of the prostate over time.

Using this model, two episodes of prostate-specific inflammation were induced to study the effects of inflammation in a model that develops subtle epithelial lesions over several months. The studies addressed the hypothesis that induced prostatitis would enhance the development of precancerous epithelial lesions. In the acute phase, prostate epithelium was highly proliferative and showed enhanced bioluminescence. However, by 4 months after inflammation, mice with previous bouts of inflammation showed similar numbers of lesions and slightly decreased average grade of lesions compared with those mice in which inflammation was not induced, although spontaneous inflammation was observed in noninduced mice. A trend toward invasion was observed at later time points in mice with induced inflammation, but average lesion grade, size of lesions, and number of lesions were unchanged between the induced and non-induced mice. Taking into consideration that *Pten*^{+/-} mice

develop spontaneous prostatitis over time, the mice were also analyzed as a single cohort, and a positive association between myeloid cell infiltration and lesion development was observed.

Materials and Methods

Mice and Genotyping

Animal experiments described in this study were approved by the Purdue University Animal Care and Use Committee. The *C57/Luc/Pten^{-/-}* mouse model resulted from interbreeding PB-Cre4⁺ mice [B6.Cg-Tg(Pbsn-cre)4Prb], *Pten^{fl/fl}* mice (C;129S4-*Pten^{tm1Hwu}/J*), and ROSA26-LSL-Luc mice [FVB.129S6 (B6)-*Gt (ROSA)26Sor^{tm1(Luc)Kael}/J*], and backcrossing the resulting mice with albino C57BL/6 mice (*C57BL/6J-Tyrc-2J/J*), as previously described.²¹ These mice were interbred with POET-3 mice, a previously described model of prostatitis, to obtain P3⁺*Pten^{-/-}* mice containing the POET-3 transgene; PB Cre, floxed alleles of *Pten*; and prostate luciferase expression.²⁰ Genotypes needed for this study were generated via the speed expansion service at The Jackson Laboratory (Bar Harbor, ME), where sperm from *C57/Luc/Pten^{-/-}* and *C57/Luc/Pten^{+/-}* mice also hemizygous for the POET-3 transgene were used to fertilize ova from albino C57BL/6 mice (*C57BL/6J-Tyrc-2J/J*). The resulting mice were either hemizygous (P3⁺) or negative (P3⁻) for the POET-3 transgene, had two intact *Pten* alleles (*Pten^{+/+}*) or one allele of *Pten* floxed (*Pten^{+/-}*), were hemizygous for PB-Cre (PB-Cre⁺), and were hemizygous for ROSA26-LSL-Luc (Luc⁺). Mice were genotyped for the presence of all genetic mutations, as previously described.²¹

In Vivo Bioluminescence Imaging

Mice for *in vivo* imaging were anesthetized with a combination of ketamine and xylazine and were dosed intraperitoneally with 0.15 mg/g of body weight D-Luciferin firefly potassium salt (Gold Biotechnology, St. Louis, MO) dissolved in Dulbecco's phosphate-buffered saline. Mice were placed in dorsal recumbency, and bioluminescent signal was imaged with the IVIS Lumina II (Caliper Life Sciences, Hopkinton, MA). Bioluminescence was collected by using a 2-minute exposure at 5-minute intervals for up to 30 minutes. Bioluminescence was measured in photons flux/second within a region of interest, defined as 8% maximum signal by using the Living Image software version 4.0 (Caliper Life Sciences). The single, peak bioluminescent signal obtained over the 30-minute imaging session for each mouse was used in data analysis.

Induction of Prostatitis

Splenocytes were isolated from male *Rag1^{-/-}* OT-I mice [a cross between B6.129S7-*Rag1^{tm1Mom}/J* mice obtained from The Jackson Laboratory and Tg(TcraTcrb) 1100Mjb mice

obtained as a gift from Dr. William Heath (Walter and Eliza Hall Institute, Melbourne, Australia)] and cultured at 5×10^5 /mL with 1 μ g/mL SIINFEKL (ova peptide 357-264; American Peptide Company Inc., Sunnyvale, CA) for 48 hours in RPMI 1640 medium with 10% fetal bovine serum, 5% sodium pyruvate, 5% penicillin-streptomycin, and 5% 1 mol/L HEPES. Live cells were purified by Fico/Lite (Atlanta Biologicals, Norcross, GA), and 5×10^6 cells were injected intravenously.

Flow Cytometry

Single-cell suspensions of prostates were obtained by mincing the tissues in a solution of RPMI 1640 medium with 2 μ g/mL collagenase D (Roche Diagnostics, Indianapolis, IN) and digesting the tissue at 37°C for approximately 1 hour. Single-cell suspensions of splenocytes were also collected from each mouse. Cells were filtered via 35- μ m mesh cell strainer caps, washed with medium, and treated with TruStain fcX anti-CD16/32 antibody (catalog 101319; BioLegend, San Diego, CA), then labeled with the following directly conjugated anti-mouse antibodies according to the manufacturer's instructions: BioLegend peridinin chlorophyll anti-CD45 (catalog 103129), fluorescein isothiocyanate (FITC) anti-CD45 (catalog 103107), phosphatidylethanolamine (PE)/cyanine 7 anti-CD45R/B220 (catalog 103221), FITC anti-CD4 (catalog 100405), PE anti-CD11b (catalog 101207), PE/cyanine 7 anti-CD11b (catalog 101215), allophycocyanin anti-Gr-1 (catalog 108411), FITC anti-F4/80 (catalog 123107), PE anti-Fc ϵ RI α (catalog 134307), and allophycocyanin anti-CD4 (catalog 17-0042-81; eBioscience, San Diego, CA). Aliquots of sample were separated and labeled with the appropriate isotype control antibodies (BioLegend). Labeling for the intracellular antigen FOXP3 was performed with the PE-conjugated anti-FOXP3 Flow Kit (BioLegend). Analysis was performed with the FACSCanto II (BD Biosciences, San Jose, CA), and data were further analyzed with FlowJo software version 9 (TreeStar Inc., Ashland, OR).

RNA Isolation, cDNA Synthesis, and RT-PCR

Sections of each lobe of the prostate were flash frozen in liquid nitrogen and stored at -80°C before homogenization. For RNA extraction, tissues were submerged in 2 mL of TRK lysis buffer (Omega Bio-Tek Inc., Norcross, GA) and homogenized with the Tissue Tearor (BioSpec Products, Inc., Bartlesville, OK). Lysates were centrifuged, and the supernatant was collected. RNA was isolated from the supernatant by using the Total RNA isolation kit I (Omega Bio-Tek Inc.), and cDNA synthesis was performed with qScript cDNA SuperMix (Quanta BioSciences, Inc., Gaithersburg, MD). RT-PCR was performed with LightCycler 96 Real-Time PCR System (Roche Diagnostics) and PrimeTime qPCR probes (Integrated DNA Technologies, Inc., Coralville, IA) for the following genes: *I11b* (assay, Mm.PT.56a.41616450), *I12* (assay, Mm.PT.56a.11478202), *I14* (assay, Mm.PT.56a.32703659),

I15 (assay, Mm.PT.56a.41498972), *I16* (assay, Mm.PT.56a.10005566), *I110* (assay, Mm.PT.56a.13531087), *I113* (assay, Mm.PT.56a.31366752), and *I16ra* (assay, Mm.PT.58.31166746). TaqMan qPCR probes were used to detect the following genes: *Ifng* (assay, Mm00801778_m1), *Tnf* (assay, Mm00443258_m1), and *Tgfb1* (assay, MM00441724_m1). As an endogenous control the *18s* rRNA gene was detected via TaqMan Ribosomal RNA Control reagents (catalog 4308329; Applied Biosystems, Foster City, CA) and used for normalization. Relative amounts of mRNA were calculated as $2^{-(Ct \text{ gene of interest} - Ct \text{ 18s rRNA})}$, where Ct is the threshold cycle value.

Histology and Digital Slide Analysis

Prostate tissue was fixed with 10% neutral-buffered formalin for 24 to 48 hours, followed by routine tissue processing and paraffin embedding. A representative 5- μ m section of each of the four lobes was obtained and stained with hematoxylin and eosin (H&E). Slides were digitized with an Aperio Digital Slide Scanner (Leica, Wetzlar, Germany), and slides were analyzed by two board-certified veterinary pathologists (G.N.B. and P.W.S.) and annotated with ImageScope software version 11.2.0.780 (Leica). Individual mouse prostatic intraepithelial neoplasia (mPIN) and carcinoma lesions were outlined and measured with the ImageScope software. Immunohistochemical analysis was performed by using either the nuclear version 9 or the membrane version 9 algorithms, depending on the localization of the labeling. Average lesion grade was obtained by calculating as follows:

$$\begin{aligned} & [(\text{Number PIN I lesions} \times 1) + (\text{Number of PIN II lesions} \times 2) \\ & + (\text{Number of PIN III lesions} \times 3) \\ & + (\text{Number of carcinoma lesions} \times 4)] / \text{Total number of lesions.} \end{aligned} \quad (1)$$

A grading scheme modified from previously published schemes was developed and used to separate mPIN lesions into three separate grades (PIN I, II, III); criteria for carcinoma were adapted from the Bar Harbor meeting of the Mouse Models of Human Cancer Consortium Prostate Pathology Committee.^{22–24} A three-tier grading scheme for histologic presence of prostatic inflammation was modified from an existing grading scheme; each lobe was scored individually, and a sum of the scores was used as the total prostate inflammation.²⁵

Immunohistochemistry

For anti-Ki-67 and anti-Bcl-2, tissue sections were deparaffinized, rehydrated, submerged in decloaker solution (Biocare Medical, Concord, CA), and heated to 96°C for 20 minutes by using a laboratory microwave (Ted Pella, Inc., Redding, CA). Sections were then treated with 3% hydrogen peroxide, protein block solution (Dako, Carpinteria, CA), primary antibody (anti-Ki-67 sp6 clone, anti-Bcl-2 E17

clone; Abcam Inc., Cambridge, MA), peroxidase-linked polymeric anti-rabbit antibody (Dako), and finally 3,3'-diaminobenzidine substrate; washes with tris-buffered saline that contained 0.5% Tween 20 were conducted between each step. Slides were counterstained with hematoxylin. For anti-p-AKT, tissue sections were deparaffinized, rehydrated, submerged in antigen unmasking solution (Vector Laboratories, Burlingame, CA), heated to 121°C in a benchtop autoclave (2100-Retriever; Prestige Medical, Northridge, CA), and allowed to cool to room temperature. Sections were pretreated with 3% H₂O₂, then incubated with primary antibody (anti-p-AKT serine 473; Cell Signaling Technology Inc., Danvers, MA) and anti-rabbit secondary antibody (BA-1000; Vector Laboratories). Sections were incubated with Vectastain Elite ABC reagent (Vector Laboratories) and peroxidase substrate solution (Vector Laboratories), followed by hematoxylin counterstain. Appropriate target-specific positive and negative control tissues were used.

Cell Sorting

A previously published protocol for isolation of prostate epithelia was followed.²⁶ Briefly, minced prostate tissue was digested with 1 μ g/mL collagenase-I in RPMI 1640 medium containing 10% fetal bovine serum for 2 hours, after trypsinization at 37°C to isolate cells. The suspensions were passed through 20-gauge needles three to five times and 40- μ m cell strainers. To enrich prostate epithelial cells, isolated cells were incubated with fluorescence-conjugated specific antibodies as follows: Sca1-allophycocyanin (catalog 108112; BioLegend), CD49f-PE (catalog 12-0495-83; eBioscience), CD45-FITC (catalog 103108; BioLegend), and CD31-FITC (catalog 553372; BD Biosciences).²⁷ CD45⁻CD31⁻Sca1⁺CD49f⁺ (prostate progenitors), CD45⁻CD31⁻Sca1⁻CD49f⁻ (luminal cells), and CD45⁻CD31⁻Sca1⁻CD49f⁺ (basal cells) were collected via live cell sorting with the use of a FACSAria (BD Biosciences).

Western Blot Analysis

Cell lysates were prepared by addition of RIPA lysis buffer (Rockland Immunochemicals, Inc., Gilbertsville, PA) containing 1 \times protease inhibitor cocktail (catalog P8340; Sigma-Aldrich, St. Louis, MO), 1 \times Phosphatase Arrest I (G-Biosciences, St. Louis, MO), 1 mmol/L phenylmethylsulfonyl fluoride, and 0.1% Triton X-100. Protein concentrations were determined with Bradford reagent (catalog B6916; Sigma-Aldrich) according to the manufacturer's instructions by using dilutions of 2 mg/mL bovine serum albumin (Thermo Scientific, Waltham, MA) to produce a standard curve for each experiment. Approximately 30 to 40 μ g of protein per sample was loaded into wells for electrophoresis. Western blot analyses were performed by probing polyvinylidene difluoride membranes with the following antibodies: anti- β -actin clone 8H10D10, anti-phospho-I κ B (14D4) rabbit monoclonal antibody

2859, and anti-phospho-I κ B (44D4) rabbit monoclonal antibody 4812 (Cell Signaling Technology Inc.).

Statistical Analysis

Statistical analyses were performed with Prism version 5.04 (GraphPad Inc., La Jolla, CA). Student's *t*-test and analysis of variance were used in cases of data with expected normal distribution, with Mann-Whitney test used in cases of non-normal distribution. Correlations between sets of continuous data were analyzed by fitting simple linear regression. Statistical significance was considered with $P < 0.05$.

Results

Bioluminescence and Cell Proliferation Increase during the Acute Phase of Prostatitis

To study prostatitis and its potential effects on prostate cancer formation, a previously described model of inducible CD8⁺ T-cell-driven prostatitis, the POET-3 mouse,^{20,28} was crossed with a prostate-specific *Pten*-deficient model of prostate cancer formation that included the *ROSA26* luciferase allele to allow *in vivo* monitoring of prostate size²¹ (Figure 1A). Both mouse models were previously backcrossed onto the C57Bl/6 background to ensure genetic homogeneity. Once the POET-3/C57/Luc/*Pten*^{-/-} mice were available, adequate numbers of mice for experimentation were generated with The Jackson Laboratory's speed expansion service. Speed expansion generated four genotypes for study: POET-3⁺/C57/Luc/*Pten*^{+/-} (designated P3⁺*Pten*^{+/-}), POET-3⁻/C57/Luc/*Pten*^{+/-} (designated P3⁻*Pten*^{+/-}), POET-3⁺/C57/Luc/*Pten*^{+/+} (designated P3⁺*Pten*^{+/+}), and POET-3⁻/C57/Luc/*Pten*^{+/+} (designated P3⁻*Pten*^{+/+}). Thus, mice were generated with the ability to form epithelial lesions (*Pten*^{+/-}) and with and without the transgene that allows inducible inflammation (POET-3). For comparison, mice with intact *Pten*^{+/+} with and without the POET-3 transgene were also generated.

At 12 weeks of age, all genotypes of mice had similar amounts of bioluminescence, which increased gradually over time (Figure 1, C and D). At weeks 13 and 18 all mice received activated OT-I cells via adoptive transfer (Figure 1B). Prostatitis was induced only in POET-3⁺ mice as previously described.²⁰ Groups of 10 mice (5 P3⁺*Pten*^{+/-}, 5 P3⁻*Pten*^{+/-}) or 8 mice (4 P3⁺*Pten*^{+/+} and 4 P3⁻*Pten*^{+/+}) were euthanized and evaluated at 4, 8, and 12 months after induction of prostatitis (Figure 1B). Bioluminescent imaging was performed every 1 to 2 weeks during the study. P3⁺*Pten*^{+/+} mice with induced prostatitis had significantly increased ($P < 0.001$) bioluminescence in the 2 weeks after each instance of adoptive transfer of OT-I T cells; however, bioluminescence normalized soon after each episode and remained similar in each group for the remainder of the study (Figure 1C). In contrast, P3⁺*Pten*^{+/-} mice had significantly increased bioluminescence ($P < 0.001$) immediately after the first adoptive transfer of OT-I T cells at 13 weeks, which persisted until the second adoptive transfer of

T cells at 18 weeks (Figure 1D). Interestingly, the second episode of prostatitis resulted in a greater increase in bioluminescence compared with the first, suggesting enhanced epithelial cell proliferation after repeated episodes of inflammation (Figure 1D). Prostatitis was verified via histopathology, which showed diffuse interstitial infiltration of lymphocytes, with fewer numbers of macrophages and neutrophils throughout prostates of P3⁺*Pten*^{+/-} mice after adoptive transfer of OT-I T cells, with no detectable inflammation in P3⁺*Pten*^{+/-} mice before adoptive transfer and P3⁻*Pten*^{+/-} mice after adoptive transfer (Figure 2A). Immunohistochemical labeling for Ki-67 showed a significant increase in epithelial cell proliferation in all lobes of the prostates of P3⁺*Pten*^{+/-} mice ($P < 0.0001$) compared with both P3⁺*Pten*^{+/-} mice before adoptive transfer of OT-I T cells and P3⁻*Pten*^{+/-} also challenged with OT-I T cells (Figure 2B). Approximately 50% of prostate epithelial cells labeled positively with Ki-67 in P3⁺*Pten*^{+/-} mice after induction of inflammation, suggesting CD8⁺ T-cell-driven prostatitis was a strong signal for epithelial cell proliferation. Immunohistochemical labeling of phosphorylated Akt (p-Akt) was used as an indicator of lesion development in these mice, as previously described, and areas of p-Akt⁺ epithelium were increased ($P < 0.01$) in the lateral lobes of mice during the acute phase of prostatitis (Figure 2C).²¹ Some differences were observed in cell proliferation, with decreased proliferation in the ventral lobe, and Akt labeling, with increased labeling in the lateral lobe. Differences were likely not due to the amount of inflammation, because all lobes were shown to have similar inflammatory infiltrate in this model.²⁰ Differences could be a result of an as yet undescribed difference in epithelial cell biology between different prostate lobes in the mouse. Taken together, the above results indicated that severe prostatitis in P3⁺*Pten*^{+/-} mice lead to epithelial cell hyperplasia in the acute phase of inflammation and initial early expansion of multifocal areas of epithelium.

Experimentally Induced Prostatitis Does Not Translate into Increased Incidence, Size, or Grade of Epithelial Precursor Lesions

To test our hypothesis that induced inflammation promotes enhanced carcinogenesis in an environment permissive to cell proliferation, five P3⁺*Pten*^{+/-} and five P3⁻*Pten*^{+/-} mice were sacrificed at 4, 8, and 12 months after induction of prostatitis. At each time point, prostate tissue was collected and examined histologically. A grading scheme modified from previously published schemes was developed and used to separate mPIN lesions into the following three separate grades: PIN I, II, and III, with PIN III being the most severe of the precursor lesions observed.^{22,23} Biological differences in the grading scheme were validated via immunohistochemical labeling for Ki-67, in which the proliferative index was increased with higher grades (see *PIA-Like Lesions Are Present in Areas of Inflammation and Fibrosis*). Lesions were counted, graded, and measured in each lobe. As expected from previously published data that used the C57/Luc/*Pten*^{+/-}, lesion development was slow, with

few instances of mPIN at the 4-month time point (30 weeks of age) and only rare instances of carcinoma developing in the 12-month group (60 weeks of age) (Figure 3A).²¹ At 4 months after induction of prostatitis, the incidence of epithelial lesions did not differ between P3⁺*Pten*^{+/-} and P3⁻*Pten*^{+/-} mice (Figure 3B), and the average grade of mPIN lesions was lower in P3⁺*Pten*^{+/-} mice ($P = 0.02$), suggesting that prostatitis may have influenced or slowed lesion development in these mice (Figure 3C). By 8 and 12 months after inflammation, incidence of epithelial lesions and average grade of lesions were statistically similar in both groups of mice (Figure 3, B and C). Similarly, the size of PIN I and PIN II lesions did not differ between the two groups of mice at 4, 8, or 12 months after inflammation (Figure 3D and data not shown). No differences were detected between the sizes of PIN III lesions, although there were small total numbers of PIN III lesions and large variation between PIN III sizes (data not shown).

In contrast to mice with loss of one allele of *Pten*, only rare instances of epithelial lesions were observed the P3⁺*Pten*^{+/+}

and P3⁻*Pten*^{+/+} mice (Supplemental Figure S1A). However, an interesting trend toward the presence of hyperplastic lesions was observed in the P3⁺*Pten*^{+/+} mice, with one of three P3⁺ mice developing at least one instance of hyperplasia at 4 months after inflammation and no mice developing lesions in the P3⁻ group at 4 months (data not shown). Hyperplastic lesions were observed in a single P3⁺*Pten*^{+/+} mouse at 8 months after inflammation, but lesions were not observed in the P3⁻*Pten*^{+/+} mouse group (data not shown). By 12 months after induction of inflammation, three mice in the P3⁻*Pten*^{+/+} group had instances of hyperplasia, with no hyperplasia observed in P3⁺*Pten*^{+/+} mice; however, at least one instance of PIN I was seen in the previously inflamed mice (Supplemental Figure S1A).

Experimentally Induced Prostatitis May Promote Development of Invasive Lesions

Although experimental induction of prostatitis did not result in an increased incidence or higher grade of epithelial

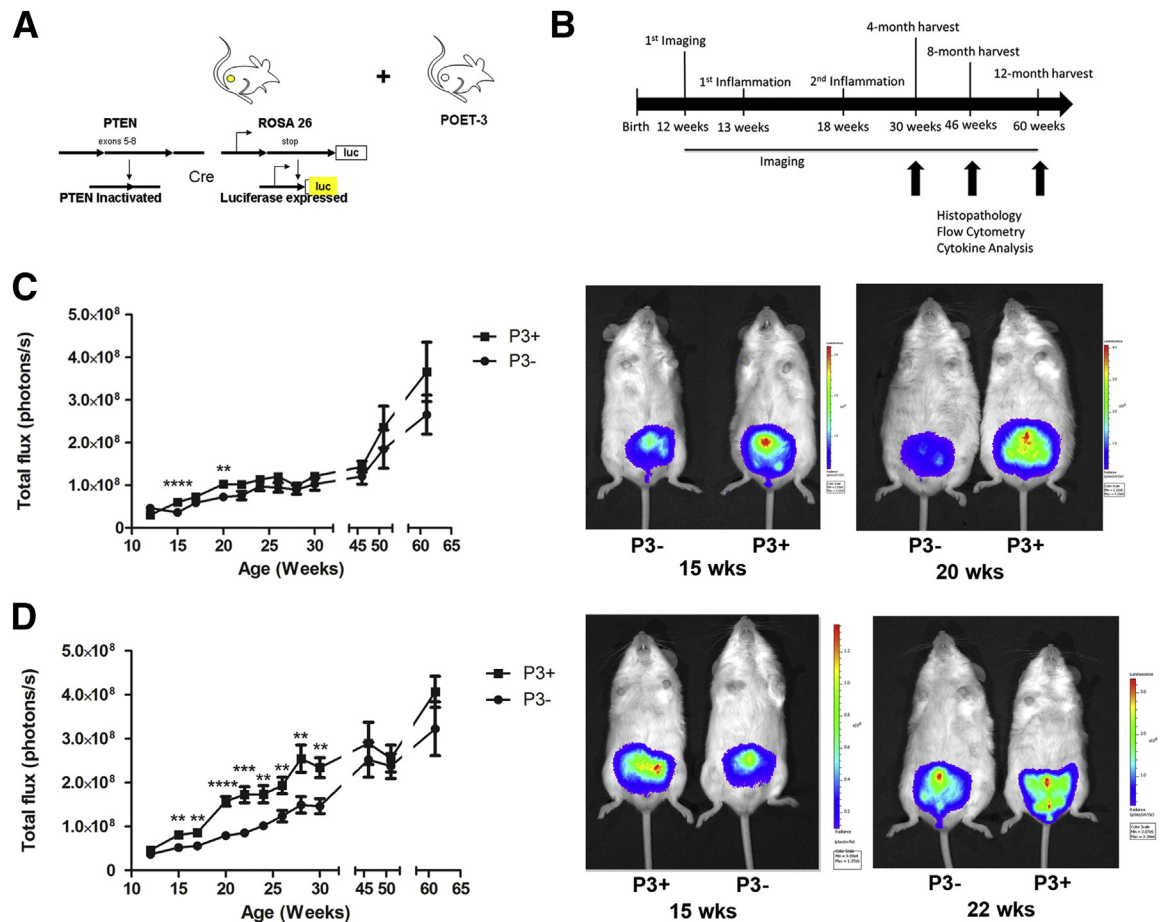


Figure 1 Bioluminescence increased with induction of prostatitis. **A:** A schematic shows the two major mouse models that were crossed for this study: the C57/Luc/*Pten*^{-/-} model of prostate carcinogenesis that contains Cre recombinase driven by the prostate-specific promoter probasin, luciferase expression in the prostate; and prostate-specific inactivation of *Pten* was crossed with the POET-3 model, allowing for controlled induction of autoimmune prostatitis. **B:** Experimental timeline shows ages of treatments and timing of tissue harvests. **C:** Bioluminescence of P3⁺*Pten*^{+/+} mice increased transiently after induction of prostatitis. **D:** Bioluminescence increased in the weeks after induction of prostatitis in P3⁺*Pten*^{+/-} mice. Data are expressed as means \pm SEM (C and D). $n = 12$ to 14 early time points (C); $n = 4$ later time points (C); $n = 15$ to 22 early time points (D); $n = 4$ to 5 later time points (D). ** $P < 0.01$, *** $P < 0.001$, and **** $P < 0.0001$, Student's t -test.

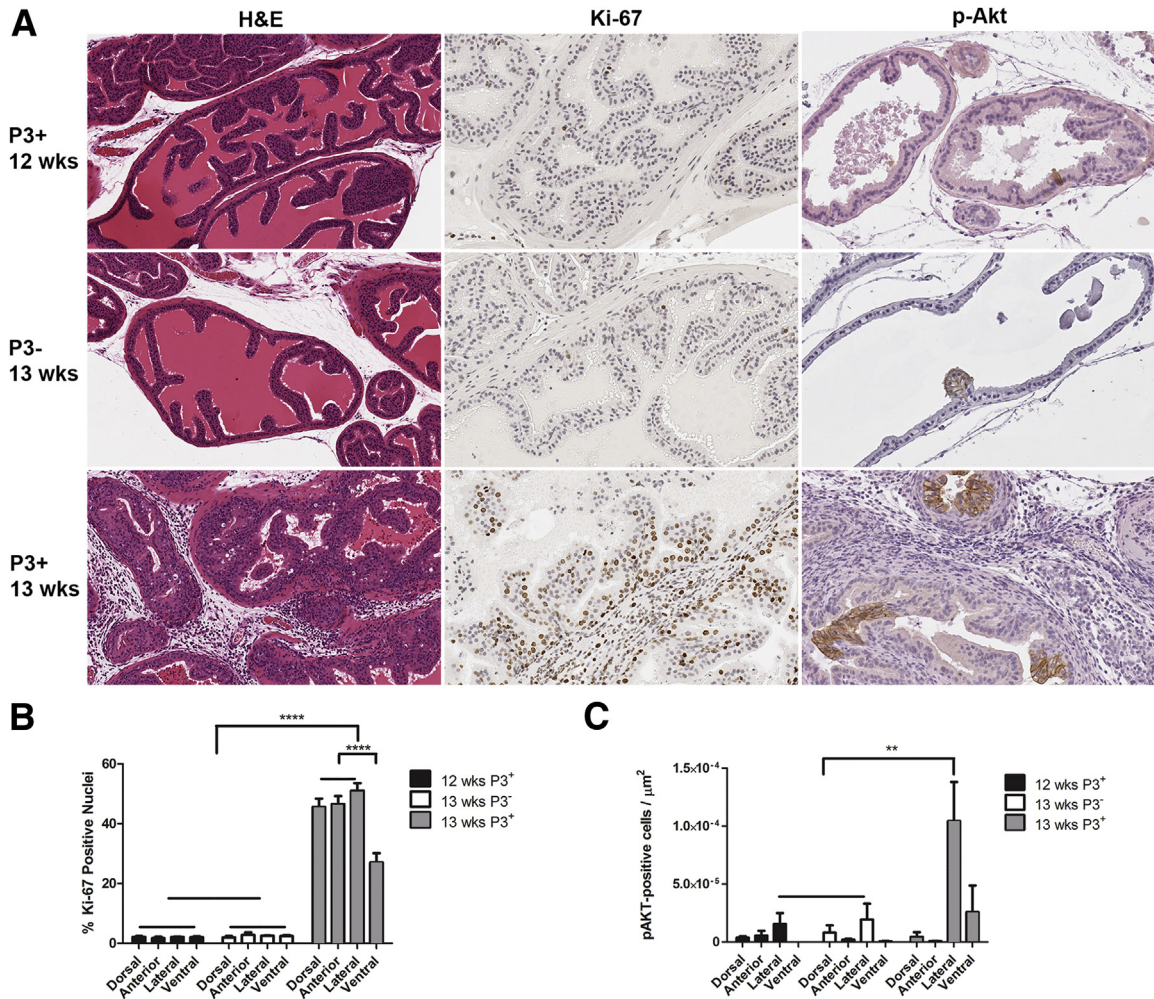


Figure 2 Prostatitis increased the percentage of dividing epithelial cells and number of cells with enhanced Akt signaling. **A:** P3⁺Pten^{+/-} before adoptive transfer of OT-I T cells at 12 weeks of age and P3⁻Pten^{+/-} mice after adoptive transfer of OT-I T cells at 13 weeks of age showed no prostatitis by H&E staining, low amounts of cell proliferation by anti-Ki-67 IHC, and few cells with enhanced phosphorylation of Akt by anti-p-Akt IHC. P3⁺Pten^{+/-} mice 6 days after adoptive transfer of OT-I T cells at 13 weeks of age showed severe prostatitis by H&E staining, high amounts of cell proliferation by anti-Ki-67 IHC, and larger areas of cells with enhanced phosphorylation of Akt by anti-p-Akt IHC. Anterior lobes shown in H&E, Ki-67 panels; lateral lobes shown in p-Akt panels. **B:** Quantification of anti-Ki-67 IHC in the three groups of mice represented in **A**. **C:** Quantification of anti-p-Akt IHC in the three groups of mice represented in **A**. Data are expressed as means ± SEM (**B** and **C**). n = 5 mice each group (**B**); n = 5 mice in Pre and P3⁻ (**C**); n = 4 mice in P3⁺ (**C**). **P < 0.01, ****P < 0.0001, one-way analysis of variance or Student's t-test. IHC, immunohistochemistry.

lesions as hypothesized, several noteworthy histologic observations were made in P3⁺Pten^{+/-} prostates. First, a trend toward increased carcinoma development was present in P3⁺Pten^{+/-} mice compared with P3⁻Pten^{+/-} mice. Carcinoma was observed only in the mice evaluated at 12 months after prostatitis induction, with two of five P3⁺Pten^{+/-} mice and one of five P3⁻Pten^{+/-} mice developing carcinoma (Figure 3E). In one P3⁺Pten^{+/-} mouse with carcinoma, the mouse was removed from the study 2 months earlier than scheduled because of acute onset of lethargy and inappetence. Grossly the prostate was enlarged, and the urinary bladder was swollen, with multiple areas of serosal hemorrhage (Figure 4A). Microscopically there were multiple mPIN lesions throughout the prostate and periprostatic suppurative inflammation. Within the wall of the urinary bladder, longitudinal sections of peripheral nerve were circumscribed by a

pleomorphic population of round-to-polygonal epithelial cells with anisocytosis, anisokaryosis, and multiple mitotic figures, interpreted as prostatic carcinoma with perineural invasion (PNI) and extraprostatic extension (Figure 4B).

PIA-Like Lesions Are Present in Areas of Inflammation and Fibrosis

In addition, 1 of 8 Pten^{+/-} mice at 8 months and 1 of 10 Pten^{+/-} mice at 12 months contained regions of the lateral lobe of the prostate in which multiple prostate glands were lined by flattened, atrophic epithelial cells (Figure 5A). Glands lined by atrophic epithelium were surrounded by extensive interstitial fibrosis and inflammation. Some affected glands were ectatic. Interestingly, some glands contained mPIN-like lesions or, in one instance, a microinvasive carcinoma lesion, despite their

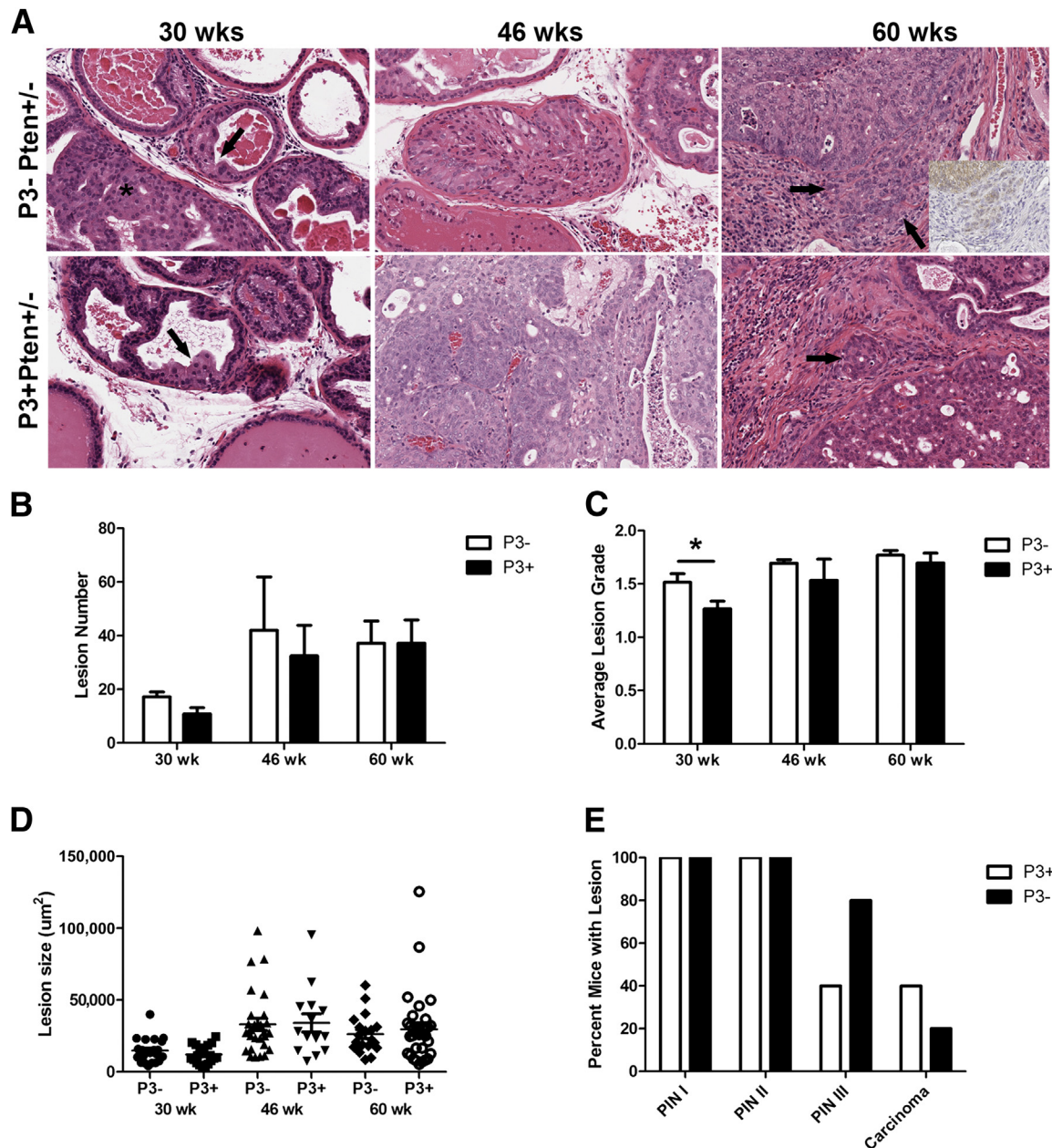


Figure 3 Experimentally induced prostatitis did not result in increased numbers or severity of epithelial lesions. **A:** Examples of epithelial lesions in P3⁺Pten^{+/-} and P3⁻Pten^{+/-} mice 30 weeks of age (4 months after induction of prostatitis), 46 weeks of age (8 months after induction), and 60 weeks of age (12 months after induction). The photomicrographs taken from H&E-stained sections represent lesions considered PIN I in the lateral lobe (in both genotypes at 30 weeks, indicated with **arrows**; adjacent PIN II lesion indicated with **asterisk**), PIN III in the dorsal lobe (in both genotypes at 46 weeks), and PIN III with adjacent foci of invasion in the lateral lobe (both genotypes at 60 weeks). Foci of carcinoma are indicated with **arrows** in 60 weeks column. **Inset** at 60 weeks shows p-Akt IHC, showing epithelial cells invading surrounding stroma. **B:** Total lesion number did not differ between P3⁺Pten^{+/-} and P3⁻Pten^{+/-} mice at 4, 8, and 12 months after induction of inflammation. Lesions from all four prostate lobes in each mouse were tallied and combined. **C:** Average lesion grade for all prostate lobes was obtained for each mouse. Mice with induction of prostatitis have decreased average lesion grade at 4 months after induction compared with mice without induction of inflammation. Both groups had similar lesion grades at 8 and 12 months after induction. **D:** Size of PIN I lesions in the dorsal lobe of the prostate did not differ between P3⁺Pten^{+/-} and P3⁻Pten^{+/-} mice at 4, 8, and 12 months. Size of other lesion types in the other prostate lobes showed similar results. **E:** Percentage of mice with each of the mPIN lesion grades and carcinoma was similar after induction of prostatitis (60 weeks), with more P3⁺Pten^{+/-} showing carcinoma. Data are expressed as means \pm SEM (**B** and **C**); error bars represent SEM (**D**). $n = 4$ to 5 mice each group (**B–D**); $n = 5$ mice each group (**E**). * $P < 0.05$. Mann-Whitney test. IHC, immunohistochemistry.

quiescent morphologic appearance (Figure 5A). Given the morphologic similarity of these lesions to the previously described proliferative inflammatory atrophy (PIA) lesions observed in human prostates, further characterization of the

nature of these lesions was initiated.^{29,30} PIA lesions in men have been shown to have increased proliferative capacity and labeling of antiapoptotic proteins, such as Bcl-2.²⁹ Immunohistochemical labeling for Ki-67, Bcl-2, and p-Akt was

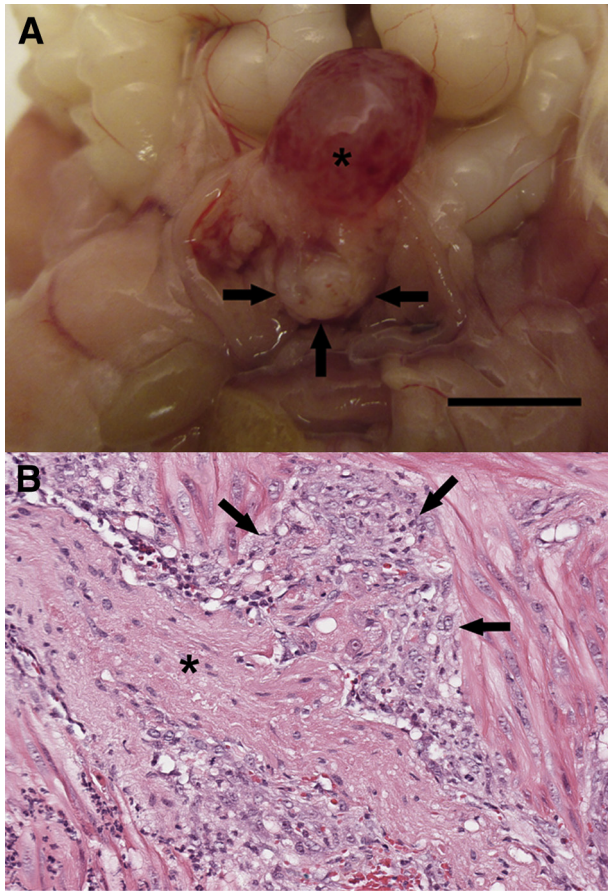


Figure 4 PNI of prostate carcinoma occurred in a single $P3^{+}Pten^{+/-}$ mouse approximately 10 months after induction of inflammation. **A:** Gross image demonstrates hemorrhagic cystitis (asterisk) and prostatomegaly with hemorrhage (arrows) in a $P3^{+}Pten^{+/-}$ mouse. **B:** Photomicrograph of a H&E-stained section of prostate and adjacent urinary bladder wall shows a peripheral nerve (asterisk) surrounded by a monomorphic population of carcinomatous epithelial cells (arrows) exhibiting nuclear pleomorphism, anisokaryosis, anisocytosis, and increased mitotic rate. Scale bar = 1 cm.

performed on sections of prostate containing the PIA-like lesions (data not shown and Figure 5A). Although Bcl-2 was not expressed in these lesions, the proliferative index of affected epithelium was found to be approximately seven times higher than normal epithelium, was higher than all grades of mPIN, and was equally as high as instances of carcinoma (Figure 5B). Individual glands in other lobes of prostates from $P3^{+}Pten^{+/-}$ and $P3^{-}Pten^{+/-}$ mice in the 8- and 12-month time points had focal areas of atrophied epithelium but were differentiated from the aforementioned lesions by decreased proliferative indices and lack of surrounding interstitial fibrosis and inflammation.

Experimentally Induced Prostatitis Leads to Increased Numbers of Lymphoid Cells in Early Time Points; Spontaneous Prostatitis Tends to Include Increased Numbers of Myeloid Cells

To better understand the type and severity of prostatitis occurring at these different time points, prostate homogenates were

analyzed via flow cytometry with the use of phenotypic markers of leukocyte subsets. Four months after induction of prostatitis, $P3^{+}Pten^{+/-}$ mice had a trend toward increased percentage of $CD45^{+}$ cells in the prostate ($P = 0.06$), with the percentage of $CD45^{+}$ cells becoming more even between the two groups at 8 and 12 months after inflammation, with the exception of a single outlier in the $P3^{-}$ 12-month group (Figure 6A). The percentage of lymphoid subsets infiltrating prostates at 4 months after induction of inflammation was increased for $CD8^{+}$ T cells in mice that were previously inflamed ($P = 0.055$); when correcting for the percentage of $CD45$ infiltration in each mouse, trends toward increased numbers of

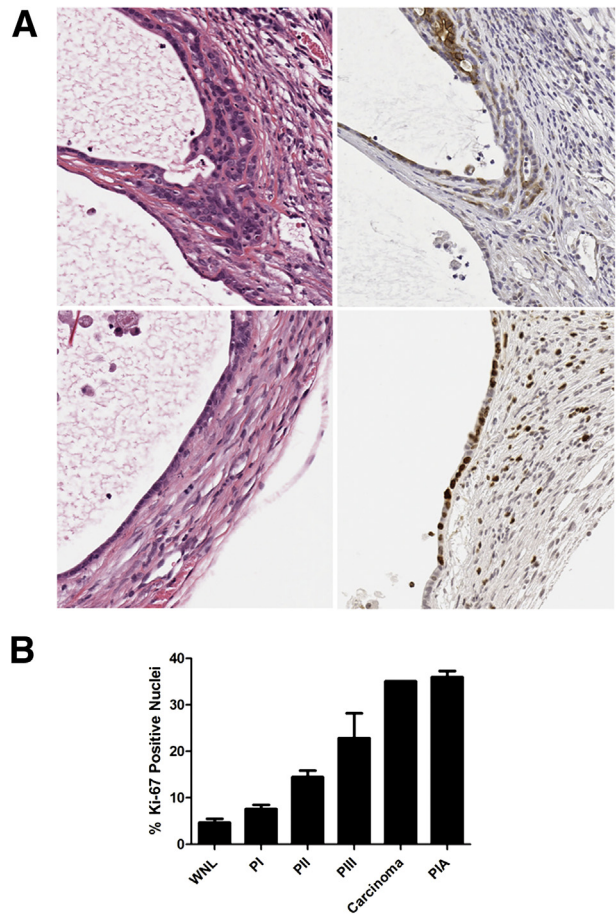


Figure 5 PIA-like lesions developed in two $Pten^{+/-}$ mice, one at 8 months and one at 12 months after induction of inflammation. **A:** Photomicrographs of H&E-stained sections of lateral prostate from a $P3^{+}Pten^{+/-}$ mouse (left column). Epithelium lining dilated glands shows features of PIA, with flattened, low cuboidal cells that contain scant cytoplasm. In the top panels, epithelial cells show the early stages of microinvasion, dissecting through the basement membrane and underlying layers of collagen. H&E, top right; anti-p-Akt, top left. Stretches of affected epithelium have a high proliferation rate, with increased cells positive for anti-Ki-67 (bottom right panel). **B:** PIA-like lesions show higher proliferative rates than normal epithelium and various amounts of precancerous epithelium lesions from mice 12 months after induction of inflammation. Multiple lesions were sampled for each category in each mouse. Data are expressed as means \pm SEM (B). $n = 10$ mice in WNL and PIN groups (B); $n = 1$ mouse in carcinoma group (B); $n = 2$ mice in PIA group (B). WNL, normal epithelium.

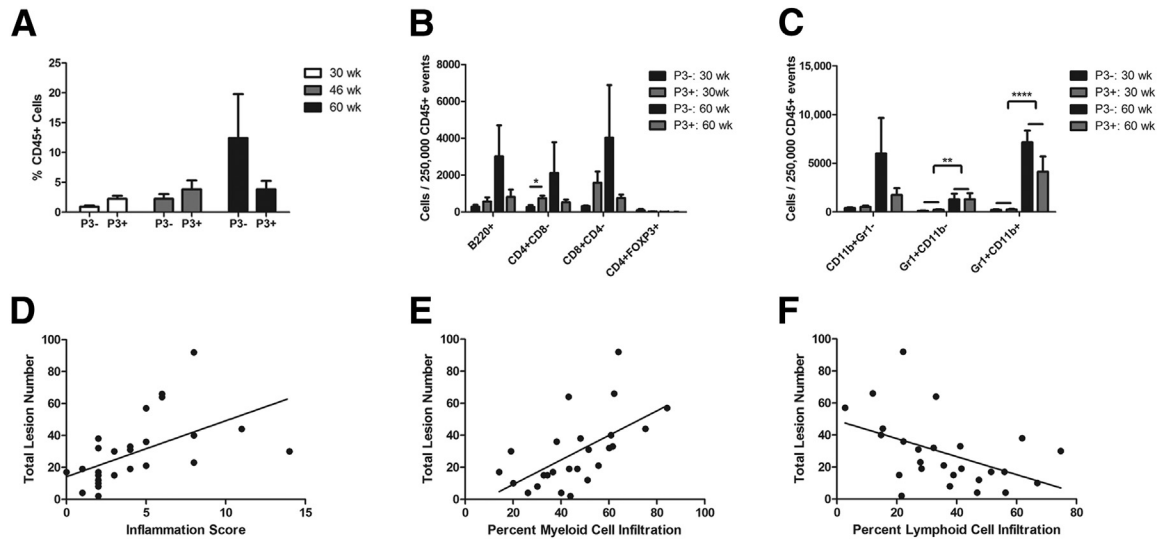


Figure 6 Lesion development was positively correlated with myeloid cell infiltration. **A:** Percentage of total CD45⁺ events was measured in prostate homogenates of P3⁺Pten^{+/-} and P3⁻Pten^{+/-} mice at various time points via flow cytometry. **B:** CD45⁺ events were further classified according to various subsets of lymphoid cells. Data are displayed as number of cells bearing the indicated antigens per amount of CD45⁺ cells. At 4 months after induction of prostatitis (30 weeks), P3⁺Pten^{+/-} mice showed a trend toward greater numbers of lymphoid cells, with significantly more CD4⁺ cells. **C:** Myeloid subsets were also investigated; data are displayed as number of cells bearing the indicated antigens per amount of CD45⁺ cells. P3⁺Pten^{+/-} and P3⁻Pten^{+/-} mice showed increases in all myeloid subsets over time, with significantly more Gr1⁺ and Gr1⁺CD11b⁺ cells at 12 months after induction of prostatitis. **B** and **C:** The first two bars in each subset represent the 30-week timepoint, while the last two bars in each subset represent the 60-week timepoint. **D:** Histologically determined inflammation score was positively correlated with lesion development in a combined cohort of P3⁺Pten^{+/-} and P3⁻Pten^{+/-} mice at all time points. $P = 0.0035$, $R^2 = 0.2932$, linear regression analysis. **E:** Lesion development was positively correlated with the percentage of total leukocytes (CD45⁺ cells) bearing the myeloid markers CD11b and Gr-1. $P = 0.0002$, $R^2 = 0.4635$, linear regression analysis. **F:** Lesion development was negatively correlated with the percentage of total leukocytes (CD45⁺ cells) bearing CD4, CD8, or B220. $P = 0.0168$, $R^2 = 0.2158$, linear regression analysis. Data are expressed as means \pm SEM (**A–C**). $n = 4$ to 5 mice each group (**A–C**). * $P < 0.05$, ** $P < 0.01$, and **** $P < 0.0001$, Student's *t*-test.

CD8⁺, CD4⁺, and B220⁺ cells in P3⁺ mice were observed, with significantly increased numbers of CD4⁺ cells ($P = 0.03$) in previously inflamed mice (Supplemental Figure S2A and Figure 6B). The percentage of Gr1⁺CD11b⁻ cells was significantly increased in P3⁻Pten^{+/-} mouse prostates compared with P3⁺ mice ($P = 0.028$), with trends toward increased CD11b⁺Gr1⁻ and CD11b⁺Gr1⁺ cells in P3⁻ mice as well at the 4-month time point (Supplemental Figure S2B). Taken together, these results suggest that mice with repeated episodes of inflammation have an infiltrate biased toward lymphoid cells, whereas the P3⁻ mice with spontaneous prostatitis had relatively greater percentages of myeloid cell infiltration. At both 8 and 12 months after induction of prostatitis, no statistically significant differences between percentages or numbers of infiltrating leukocytes existed between the P3⁺ and P3⁻ groups, suggesting that inflammation had normalized between both groups (Supplemental Figure S2, C and D, and Figure 6, B and C). However, total numbers of myeloid cells, specifically Gr1⁺CD11b⁺ cells, increased over time in both groups (Figure 6C and Supplemental Figure S2D).

Lesion Development across Both P3⁺Pten^{+/-} and P3⁻Pten^{+/-} Mice Is Positively Correlated with Infiltration of Myeloid Cells

Although the development of PNI may be associated with previous episodes of experimentally induced prostatitis, the

development of lesions, including PIN III, PIA, and carcinoma, occurred in both P3⁺Pten^{+/-} and P3⁻Pten^{+/-} mice. As previously reported, we observed the development of prostatitis and interstitial fibrosis in close proximity to many of these lesions.²¹ We documented a steady increase in the percentage of total CD45⁺ cells recovered from whole prostate homogenates in both groups of mice, indicating that spontaneous prostatitis occurs in Pten^{+/-} mice even without previous episodes of induced prostatitis (Figure 6A). Given the lack of association of lesion incidence or grade with induction of inflammation, we hypothesized that the severity of lesions was linked to the presence of inflammation generally, not just the CD8-driven inflammation induced in mice with the POET-3 transgene. Thus, mice were analyzed *post hoc* as a single cohort without regard to the presence or absence of POET-3, via simple linear regression. In this study, both lesion incidence and lesion grade were positively correlated with inflammation, whether measured by flow cytometry and the presence of CD45 or by histologic grade as inflammation score ($P = 0.0035$, $R^2 = 0.2932$; data not shown) (Figure 6D). As mentioned in the previous subsection, changes in the cellular composition of prostatitis occurred over time, with P3⁺Pten^{+/-} mice gradually moving from a more lymphocyte-based prostatitis to inflammation that includes some lymphocytes and various myeloid subsets. Literature linking inflammation and cancer supports the idea that myeloid-based inflammation, which includes macrophages and neutrophils, may be the more detrimental type of

inflammation in reference to promotion of carcinogenesis.^{31,32} When a model was fit by using myeloid cell infiltration (any cell with the presence of CD11b, Gr1, or both), lesion incidence was positively correlated ($P = 0.0015$, $R^2 = 0.3604$) with the percentage of myeloid cell infiltrate in the prostate (Figure 6E). The best fit ($P = 0.0002$, $R^2 = 0.4635$) was obtained if only those myeloid cells bearing both CD11b and Gr1 were used (data not shown). Conversely, when considering lymphoid infiltrate (any cell bearing CD8, CD4, or B220), lesion incidence was negatively correlated ($P = 0.0168$, $R^2 = 0.2158$) (Figure 6F). Considering previous data indicating lower lesion grade and higher numbers of CD4⁺ lymphocytes in the early 4-month postinflammation group, these results suggested high-grade epithelial lesions in the prostate may be associated with the presence of myeloid cell infiltrate.

Cytokine expression was also considered in the context of inflamed versus less-inflamed mice, as measured via histopathologic grading; this analysis was done with a combined cohort including mice with induced and non-induced inflammation. Although no statistically significant differences were observed between P3⁺Pten^{+/-} and P3⁻Pten^{+/-} mice for cytokine expression at the 4-, 8-, and 12-month time points, mice with histologically more severe inflammation (those mice with an inflammation score of 4 or higher) had a trend toward increased IL-6 expression compared with those mice with less inflammation and fewer lesions (Supplemental Figure S3A). Cytokines that characterized the type 1 or acute inflammatory response had similar expression between inflamed and less-inflamed mice, and amounts of cytokines that typically associated with type 2 inflammation were typically lower in inflamed mice compared with less-inflamed mice at the 12-month time point (Supplemental Figure S3B). The IL-6 receptor subunit α did not follow the trend of IL-6, with similar mRNA expression between inflamed and less-inflamed mice at 12 months of age (data not shown). Thus, as previously reported in other studies of cytokines and prostate carcinogenesis, IL-6 may play a role in the development of prostate cancer.

Acute and Chronic Inflammation in the Prostates of P3⁺Pten^{+/-} Mice Leads to Decreased I κ B

Given that p-Akt has been linked to activation of the transcription factor NF- κ B in a PTEN-null prostate cancer-derived epithelial cell line and that nuclear localization of NF- κ B has been linked to biochemical recurrence of prostate cancer and tumor grade in human prostate cancer, investigation into whether NF- κ B was activated in the PTEN loss mouse model of prostate cancer may be important.^{33–35} Little has been done to link NF- κ B activation to cancer development in mouse models of prostate cancer, although constitutive NF- κ B activity has been shown in the transgenic adenocarcinoma of the mouse prostate model.³⁶ To address this question, acute prostate inflammation was induced via OT-I injection in two young (2 to 3 months old) P3⁺Pten^{+/-}

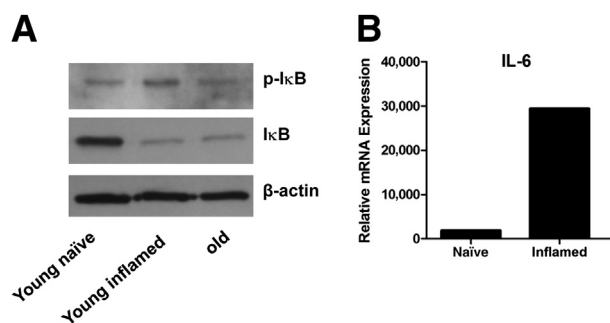


Figure 7 Inflammation in this model leads to decreased I κ B protein expression and IL-6 mRNA expression in prostate epithelial cells. **A:** Western blot analyses showed decreased I κ B protein in young mice with OT-I–induced inflammation and in chronically inflamed older mice. Phosphorylated I κ B concentrations were increased in young mice with OT-I–induced inflammation. **B:** IL-6 mRNA expression was increased in prostate epithelial cells from young mice with OT-I–induced inflammation. Data represented a pooled sample of sorted epithelial cells from two mice in each group.

mice. Nonleukocytic, nonstromal cells were collected via fluorescent-activated cell sorting in these inflamed mice, and in two young (2 to 3 months old) P3⁺Pten^{+/-} mice given phosphate-buffered saline (uninflamed) and two older (12 months old) P3⁺Pten^{+/-} mice that had not been dosed with OT-I cells. Given previous results in Figures 2 and 6, acute inflammation is present in young P3⁺Pten^{+/-} mice dosed with OT-I cells, chronic inflammation is present in older P3⁺Pten^{+/-} mice, and no inflammation was present in young phosphate-buffered saline-dosed P3⁺Pten^{+/-} mice. Western blot analysis showed decreased I κ B in both inflamed young and chronically inflamed older P3⁺Pten^{+/-} mice compared with young noninflamed mice, suggesting I κ B degradation and resulting NF- κ B nuclear localization (Figure 7A). Decreased I κ B corresponded with increased phosphorylated I κ B in inflamed young mice but not in chronically inflamed older mice (Figure 7A). Furthermore, *IL6*, a downstream target gene of activated NF- κ B, showed a many-fold increase in mRNA expression in sorted nonleukocytic, nonstromal prostate cells from young inflamed mice compared with young naive mice (Figure 7B). Taken together, these results suggested that the transcription factor NF- κ B is activated in prostate epithelium after acute, and perhaps chronic, inflammation in P3⁺Pten^{+/-} mice.

Discussion

This study was initiated to address the current discrepancies about the relation between prostatitis and prostate cancer development in the biomedical literature and to fill a need for animal models to address this question. The POET-3 mouse specifically models T-cell–driven prostate autoimmunity, whereas the C57/Luc/Pten^{+/-} mouse models a slow progression to prostate cancer, using the genetic alteration most commonly found in human prostate cancer.³⁷ Advantages of this particular model include prostate-specific

inflammation and *Pten* gene deletion, acute episodes of T-cell-driven inflammation followed by CP to mimic autoimmunity, progression of epithelial lesion development that is similar to human prostate cancer, ability to monitor prostate size *in vivo*, and a homogenous genetic background (C57BL/6).^{20,21,38}

Studies that use rodent models of prostatitis and prostate cancer development have suggested that inflammation promotes development or progression of epithelial lesions in the prostate. Coupled with additional epidemiologic evidence, these studies informed our hypothesis that prostatitis will promote the progression of epithelial lesions in this mouse model.^{16,17} The results of our study were mixed and suggest a more complex relation between inflammation and cancer development in the prostate. In the simplest setting, the P3⁺*Pten*^{+/+} mouse, early time points after induction of inflammation suggest that induced prostatitis may promote the development of hyperplastic lesions, because one of three inflamed P3⁺*Pten*^{+/+} mice at 4 months and one of four mice at 8 months after induction of prostatitis had hyperplastic epithelial lesions (Supplemental Figure S1A). Mice in the uninflamed control group did not develop histologically recognizable epithelial lesions until 12 months after treatment, suggesting that prostatitis might induce hyperplasia more quickly in normal prostate epithelium. These results are consistent with a role for inflammation in benign prostatic hyperplasia, as suggested by previous investigators.^{39–42}

Interpretation of inflammation in the P3⁻*Pten*^{+/-} and P3⁺*Pten*^{+/-} mice was more complicated, because results differed between early and late time points. In P3⁺*Pten*^{+/-} mice, the week immediately after induction of prostatitis had highly proliferative prostate epithelium, via both bioluminescence and Ki-67 immunolabeling (Figures 1 and 2). Although bioluminescence in inflamed mice remained increased above the unchallenged mice for several weeks, the mice examined at 4 months after induction of prostatitis did not have increased incidence, size, or grade of mPIN lesions. (Figure 3) In fact, when comparing the average grade of epithelial lesions across all prostate lobes between inflamed and uninflamed mice, previously inflamed mice had a lower average lesion grade. The explanation of this observation likely lies in the type of inflammation that was induced, and likely persisted, in the prostates of previously inflamed mice. Flow cytometric analysis showed trends toward higher numbers of lymphoid subsets (CD8⁺, CD4⁺, B220⁺), with statistically significantly more CD4⁺ T cells in 4-month prostates of P3⁺ mice (Figure 6). Previous characterization of the POET-3 model shows significantly enhanced expression of T helper cells type 1 (Th1) and acute inflammatory cytokines such as IL-2, IL-12, and tumor necrosis factor- α .²⁰ These early episodes of inflammation likely influenced recruitment of Th1 CD4⁺ cells, as supported by increased numbers of CD4⁺ cells at 4 months after inflammation, and may have biased the prostate microenvironment toward a less cancer-promoting type 1 inflammation. Inflammation that

developed spontaneously over this same time frame in P3⁻*Pten*^{+/-} mice was biased toward myeloid-based inflammation, which suggests a more tumor-promoting type 2 inflammatory microenvironment. Indeed, when mice from all time points are analyzed without regard for POET-3 status, lymphoid-based prostatitis was significantly negatively correlated with lesion development, whereas myeloid-based inflammation was significantly positively correlated (Figure 6). These results together suggest that episodes of Th1-based prostatitis in the P3⁺*Pten*^{+/-} mouse may be protective in reference to early mPIN development and may lend support to recently published evidence showing prostatitis as protective for development of prostate cancer.^{8,9} Much of the literature before these referenced studies relied on physician-diagnosed cases of prostatitis, of which 90% were likely cases of CP/CPPS.¹⁹ Evidence suggests that approximately one-third of CP/CPPS cases are characterized by biopsy-determined prostate inflammation, and recent studies suggest that the presence of histologically defined prostatitis is similar between men with and without symptoms of CP/CPPS.^{25,43} Many of the patients in previous studies of prostatitis and cancer development were likely diagnosed on the basis of pelvic pain and may have lacked histologic prostatitis, which makes the recent biopsy-based studies in the United States and Finland much stronger when considering true leukocytic infiltration and its relation to cancer development.

Considering the later time points in our study, 8 and 12 months after induction of prostatitis, the incidence, size, and average grade of mPIN lesions was similar across both groups of mice. However, a trend toward invasion was noted in P3⁺*Pten*^{+/-} mice, with more mice developing carcinoma. One of the weaknesses of this study was the lack of statistical power for rare events, such as carcinoma development, leading to speculation about whether previous bouts of prostatitis might have promoted invasion at later points. Because the C57/Luc/*Pten*^{+/-} phenotype includes the development of spontaneous inflammation over time, we had the opportunity to also analyze lesion development in light of development of prostatitis in general, whether it was non-induced (spontaneous) or induced inflammation. In these analyses, lesion incidence and lesion grade were clearly correlated with inflammation, with the most relevant correlation coming when infiltration of myeloid cells bearing both CD11b and Gr1 was considered. As previously mentioned, cancer development and progression are associated with specific leukocyte subsets and specific cytokine environments. Macrophages, neutrophils, and myeloid-derived suppressor cells (MDSCs) all produce substances that are considered damaging to host cell membranes and DNA, such as reactive oxygen and nitrogen species. These components might be helpful to the host if directed at tumor cells themselves, but when considering the early development of malignancy and the progression from lower grade mPIN lesions to higher grade precursor lesions and eventually invasive lesions, the products often associated with myeloid cells might be considered detrimental and tumor promoting.

Specifically, leukocytes bearing the CD11b⁺Gr1⁺ phenotype might be considered either activated neutrophils or MDSCs, both of which are known to produce damaging free radicals that promote cancer progression.⁴⁴ In addition, MDSCs may interfere with antitumor immunity via suppression of cytotoxic T cells directed toward tumor antigens.⁴⁵ Previous work by our group has shown that cells sorted from prostates of *Pten*^{-/-} mice have the capacity to suppress T-cell proliferation.²¹ We also evaluated *Pten*^{+/-} mice for MDSC-mediated suppression at 7 months of age and observed strong inhibition of T-cell proliferation (data not shown). On the basis of these observations, a portion of the CD11b⁺Gr1⁺ infiltrating cells in this report are considered MDSCs that may have contributed to lesion progression.²¹

In addition to the previous findings, two interesting and unique lesions were noted in mice from this study: PNI and PIA. Although PNI is a common occurrence in prostate cancer and has been linked to poorer prognosis in other cancers, the role of PNI in predicting prostate cancer outcome is not clear.⁴⁶⁻⁴⁸ PNI has been documented in a chemically induced rat model of prostate cancer, two mouse models using the SV40-Tag transgene, a single mouse with overexpression of human 15-lipoxygenase-1, and mice with double knockout of *Pten* and *TP53*, but it has not been documented in mice with loss of only *Pten*, to our knowledge.⁴⁹⁻⁵³ Lesions resembling PIA have not been described in mouse models of prostate cancer. A consensus report relating to interpretation of lesions in transgenic mouse models have described epithelial atrophy in mice after castration but it has not related these lesions to previous episodes of inflammation or characterized them according to their proliferative capacity.²² Interestingly, these lesions developed in prostates of *Pten*^{+/-} mice that had severe prostatitis, either from previous induction with OT-I T cells or spontaneous development. At least one report in rats and one report in mice both dosed with 2-amino-1-methyl-6-phenylimidazo (4,5-*b*) pyridine show development of prostatitis, followed by atrophic epithelial lesions, suggesting that this particular lesion may develop as a result of inflammation and partial destruction of the epithelial lining.^{54,55} Atrophic lesions in the treated rats and mice developed after prostatitis and had some degree of cellular atypia in the rats; however, proliferative indices of these lesions were not specifically assessed.^{54,55} The morphology of these lesions in *Pten*^{+/-} mice certainly seems to suggest previous injury and cell loss, as in the rat model, with flattening of epithelial cells to cover the basement membrane. With only two mice having these lesions, determination of their cause is speculative. Phosphorylation of Akt in the *Pten*^{+/-} microenvironment during the acute phase of prostatitis (Figure 2C) or during the development of spontaneous inflammation later on likely leads to phosphorylation of Bad and subsequently allows Bcl-2 to inhibit epithelial cell apoptosis during severe inflammation in our model, as occurs in animal models of prostate cancer and prostate cancer cell lines.^{56,57} Although

the pathogenesis of PIA in men is unknown, overexpression of Bcl-2 has been shown in human PIA lesions, suggesting that previous Akt signaling and/or loss of Pten, accumulation of Bcl-2, and development of PIA may be linked.

Perhaps a more interesting observation related to these lesions is that in one instance, epithelial cells arising from a PIA-like gland dissect through the basement membrane and underlying layers of collagen to exhibit early microinvasion. PIA lesions and their spatial and temporal association with high-grade PIN and prostate adenocarcinoma in men have been well documented; however, only a single publication shows a direct morphologic link between atrophic glands and carcinoma in human prostate tissue, and the lesions are not currently considered true precursors of adenocarcinoma.^{29,30,58,59} The cancer-like properties of the epithelium, including their increased proliferative capacity and resistance to apoptosis, at least in men, make them suspect as cancer precursors. Although the lesions described here differ from the human lesions in their expression of an antiapoptotic protein, their highly proliferative nature and morphologic similarities suggest that they may be analogous entities. Documented early microinvasion of the basement membrane suggests that atrophic epithelial lesions with highly proliferative capacity may indeed represent a precursor lesion to prostate carcinoma.

A final part of this study considered expression of cytokines in whole prostate homogenates. Although no statistically significant differences were observed between P3⁻*Pten*^{+/-} and P3⁺*Pten*^{+/-} mice, a trend toward increasing IL-6 expression in mice with a histologic inflammation score of 4 or greater was observed when mice of all genotypes and time points were examined. As previously mentioned, IL-6 has been one of the cytokines most indicated in prostate carcinogenesis, with evidence coming from *in vitro* studies of IL-6 and prostate cancer cell lines, increases in IL-6 in sera of patients at risk of prostate cancer development, and genetic polymorphisms in the IL-6 and IL-6 receptor genes conferring decreased risk of prostate cancer development.^{14,60,61} Although the trends we observed were not statistically significant, they support previous literature suggesting a role for IL-6 in prostate carcinogenesis. Interestingly, IL-6 has been shown to activate the phosphatidylinositol 3-kinase/Akt pathway and trigger expression of cyclin A1, with positive effects on survival in prostate cancer cell lines.⁶² Thus, chronic inflammation may promote Akt pathway activity in the prostate. Given that loss of *Pten*, and subsequent increased Akt activity, without additional inflammatory stimuli (ie, no OT-I injection) leads to prostate inflammation in this model, the fact that IL-6 can lead to further Akt stimulation could potentially establish a cycle of constant inflammation and Akt stimulation.

To add information about the pathogenesis of inflammation and cancer development in this particular model, additional experiments were undertaken to understand whether the transcription factor NF-κB was activated in prostate epithelial cells in these mice. Protein analysis

showed decreased IκB in acutely inflamed young P3⁺ *Pten*^{+/-} mice and chronically inflamed older P3⁺ *Pten*^{+/-} mice, suggesting degradation of this protein and subsequent release of NF-κB to allow nuclear localization in prostate epithelial cells. Thus, inflammation in this model seems to promote NF-κB activation, which in turn would allow a positive feed-forward process to further promoting inflammation and epithelial cell survival and proliferation.⁶³ Furthermore, *IL6*, a NF-κB target gene implicated in the progression of prostate cancer, was also found to be up-regulated in prostate epithelial cells during episodes of acute inflammation. This finding further supports that NF-κB is activated in our model after inflammation, but it also lends some insight into the source of IL-6 in the prostate microenvironment, because IL-6 was found to be up-regulated in prostate homogenates with greater inflammation (Figure 6).

Conclusions

Our study suggests that the relation between inflammation and prostate cancer is complex and depends largely on the type of inflammatory microenvironment present in the prostate and the state of the epithelium (normal or loss of *Pten*). Inflammation dominated by T cells and type 1 cytokines likely leads to slower progression of epithelial precursor lesions, even if epithelial proliferation is high after episodes of inflammation. In contrast, inflammation that includes more myeloid cells, especially CD11b⁺Gr1⁺ cells, is associated with increased incidence of mPIN and higher grade epithelial lesions. In addition, previous bouts of T-cell-driven prostatitis or development of spontaneous inflammation may lead to focal damage of epithelium that later develops into atrophic epithelium with a high rate of proliferation and the potential for invasion. Finally, IL-6, a cytokine produced both in acute inflammation and by type 2-skewed macrophages and CD4⁺ T cells, is likely important for the development of epithelial lesions in the P3⁺ *Pten*^{+/-} prostate. Further studies using this model would be beneficial to advance our understanding of the cellular and molecular components of the inflammatory response that are associated with the development and progression of prostate cancer.

Acknowledgments

We thank Renee E. Vickman, Hsing-Hui Wang, Sandra Torregrosa-Allen, and Tripti Bera for assistance with tissue harvests, mouse treatments, and mouse genotyping; Aaron Taylor for expertise in conducting bioluminescence studies; Tracy Wiegand and Carol Bain for tissue processing, slide preparation, and slide digitization; and the members of the Ratliff laboratory for helpful advice and thoughtful conversation throughout the duration of the study.

Supplemental Data

Supplemental material for this article can be found at <http://dx.doi.org/10.1016/j.ajpath.2014.08.021>.

References

- Hanahan D, Weinberg RA: Hallmarks of cancer: the next generation. *Cell* 2011, 144:646–674
- Abdel-Latif MM, Duggan S, Reynolds JV, Kelleher D: Inflammation and esophageal carcinogenesis. *Curr Opin Pharmacol* 2009, 9: 396–404
- Chiba T, Marusawa H, Ushijima T: Inflammation-associated cancer development in digestive organs: mechanisms and roles for genetic and epigenetic modulation. *Gastroenterology* 2012, 143: 550–563
- Terzic J, Grivennikov S, Karin E, Karin M: Inflammation and colon cancer. *Gastroenterology* 2010, 138:2101–2114.e5
- Roberts RO, Lieber MM, Rhodes T, Girman CJ, Bostwick DG, Jacobsen SJ: Prevalence of a physician-assigned diagnosis of prostatitis: the Olmsted County Study of Urinary Symptoms and Health Status Among Men. *Urology* 1998, 51:578–584
- Jiang J, Li J, Yunxia Z, Zhu H, Liu J, Pumill C: The role of prostatitis in prostate cancer: meta-analysis. *PLoS One* 2013, 8:e85179
- Hung SC, Lai SW, Tsai PY, Chen PC, Wu HC, Lin WH, Sung FC: Synergistic interaction of benign prostatic hyperplasia and prostatitis on prostate cancer risk. *Br J Cancer* 2013, 108:1778–1783
- Yli-Hemminki TH, Laurila M, Auvinen A, Maattanen L, Huhtala H, Tammela TL, Kujala PM: Histological inflammation and risk of subsequent prostate cancer among men with initially elevated serum prostate-specific antigen (PSA) concentration in the Finnish prostate cancer screening trial. *BJU Int* 2013, 112:735–741
- Moreira DM, Nickel JC, Gerber L, Muller RL, Andriole GL, Castro-Santamaria R, Freedland SJ: Baseline prostate inflammation is associated with a reduced risk of prostate cancer in men undergoing repeat prostate biopsy: results from the REDUCE study. *Cancer* 2014, 120: 190–196
- Shebl FM, Sakoda LC, Black A, Koshiol J, Andriole GL, Grubb R, Church TR, Chia D, Zhou C, Chu LW, Huang WY, Peters U, Kirsh VA, Chatterjee N, Leitzmann MF, Hayes RB, Hsing AW: Aspirin but not ibuprofen use is associated with reduced risk of prostate cancer: a PLCO study. *Br J Cancer* 2012, 107:207–214
- Veitonmaki T, Tammela TL, Auvinen A, Murtola TJ: Use of aspirin, but not other non-steroidal anti-inflammatory drugs is associated with decreased prostate cancer risk at the population level. *Eur J Cancer* 2013, 49:938–945
- Mahmud SM, Franco EL, Turner D, Platt RW, Beck P, Skarsgard D, Tonita J, Sharpe C, Aprikian AG: Use of non-steroidal anti-inflammatory drugs and prostate cancer risk: a population-based nested case-control study. *PLoS One* 2011, 6:e16412
- Cheng I, Witte JS, Jacobsen SJ, Haque R, Quinn VP, Quesenberry CP, Caan BJ, Van Den Eeden SK: Prostatitis, sexually transmitted diseases, and prostate cancer: the California Men's Health Study. *PLoS One* 2010, 5:e8736
- Steiner H, Godoy-Tundidor S, Rogatsch H, Berger AP, Fuchs D, Comuzzi B, Bartsch G, Hobisch A, Culig Z: Accelerated in vivo growth of prostate tumors that up-regulate interleukin-6 is associated with reduced retinoblastoma protein expression and activation of the mitogen-activated protein kinase pathway. *Am J Pathol* 2003, 162: 655–663
- Steiner H, Berger AP, Godoy-Tundidor S, Bjartell A, Lilja H, Bartsch G, Hobisch A, Culig Z: An autocrine loop for vascular endothelial growth factor is established in prostate cancer cells generated after prolonged treatment with interleukin 6. *Eur J Cancer* 2004, 40:1066–1072

16. Elkahwaji JE, Zhong W, Hopkins WJ, Bushman W: Chronic bacterial infection and inflammation incite reactive hyperplasia in a mouse model of chronic prostatitis. *Prostate* 2007, 67:14–21
17. Birbach A, Eisenbarth D, Kozakowski N, Ladenhauf E, Schmidt-Suppran M, Schmid JA: Persistent inflammation leads to proliferative neoplasia and loss of smooth muscle cells in a prostate tumor model. *Neoplasia* 2011, 13:692–703
18. Krieger JN, Nyberg L Jr, Nickel JC: NIH consensus definition and classification of prostatitis. *JAMA* 1999, 282:236–237
19. Pontari MA: Etiology of chronic prostatitis/chronic pelvic pain syndrome: psychoimmunoneuroendocrine dysfunction (PINE syndrome) or just a really bad infection? *World J Urol* 2013, 31:725–732
20. Haverkamp JM, Charbonneau B, Crist SA, Meyerholz DK, Cohen MB, Snyder PW, Svensson RU, Henry MD, Wang HH, Ratliff TL: An inducible model of abacterial prostatitis induces antigen specific inflammatory and proliferative changes in the murine prostate. *Prostate* 2011, 71:1139–1150
21. Svensson RU, Haverkamp JM, Thedens DR, Cohen MB, Ratliff TL, Henry MD: Slow disease progression in a C57BL/6 pten-deficient mouse model of prostate cancer. *Am J Pathol* 2011, 179:502–512
22. Shappell SB, Thomas GV, Roberts RL, Herbert R, Ittmann MM, Rubin MA, Humphrey PA, Sundberg JP, Rozengurt N, Barrios R, Ward JM, Cardiff RD: Prostate pathology of genetically engineered mice: definitions and classification. The consensus report from the Bar Harbor meeting of the Mouse Models of Human Cancer Consortium Prostate Pathology Committee. *Cancer Res* 2004, 64:2270–2305
23. Berman-Booty LD, Sargeant AM, Rosol TJ, Rengel RC, Clinton SK, Chen CS, Kulp SK: A review of the existing grading schemes and a proposal for a modified grading scheme for prostatic lesions in TRAMP mice. *Toxicol Pathol* 2012, 40:5–17
24. Park JH, Walls JE, Galvez JJ, Kim M, Abate-Shen C, Shen MM, Cardiff RD: Prostatic intraepithelial neoplasia in genetically engineered mice. *Am J Pathol* 2002, 161:727–735
25. Nickel JC, Roehrborn CG, O'Leary MP, Bostwick DG, Somerville MC, Rittmaster RS: Examination of the relationship between symptoms of prostatitis and histological inflammation: baseline data from the REDUCE chemoprevention trial. *J Urol* 2007, 178:896–900. discussion 900–901
26. Lukacs RU, Goldstein AS, Lawson DA, Cheng D, Witte ON: Isolation, cultivation and characterization of adult murine prostate stem cells. *Nat Protoc* 2010, 5:702–713
27. Lawson DA, Xin L, Lukacs RU, Cheng D, Witte ON: Isolation and functional characterization of murine prostate stem cells. *Proc Natl Acad Sci U S A* 2007, 104:181–186
28. Lees JR, Charbonneau B, Hayball JD, Diener K, Brown M, Matusik R, Cohen MB, Ratliff TL: T-cell recognition of a prostate specific antigen is not sufficient to induce prostate tissue destruction. *Prostate* 2006, 66:578–590
29. De Marzo AM, Marchi VL, Epstein JI, Nelson WG: Proliferative inflammatory atrophy of the prostate: implications for prostatic carcinogenesis. *Am J Pathol* 1999, 155:1985–1992
30. Putzi MJ, De Marzo AM: Morphologic transitions between proliferative inflammatory atrophy and high-grade prostatic intraepithelial neoplasia. *Urology* 2000, 56:828–832
31. DeNardo DG, Andreu P, Coussens LM: Interactions between lymphocytes and myeloid cells regulate pro- versus anti-tumor immunity. *Cancer Metastasis Rev* 2010, 29:309–316
32. Grivennikov SI, Greten FR, Karin M: Immunity, inflammation, and cancer. *Cell* 2010, 140:883–899
33. Dan HC, Cooper MJ, Cogswell PC, Duncan JA, Ting JP, Baldwin AS: Akt-dependent regulation of NF- κ B is controlled by mTOR and Raptor in association with IKK. *Genes Dev* 2008, 22:1490–1500
34. Fradet V, Lessard L, Begin LR, Karakiewicz P, Masson AM, Saad F: Nuclear factor- κ B nuclear localization is predictive of biochemical recurrence in patients with positive margin prostate cancer. *Clin Cancer Res* 2004, 10:8460–8464
35. Shukla S, MacLennan GT, Fu P, Patel J, Marengo SR, Resnick MI, Gupta S: Nuclear factor- κ B/p65 (Rel A) is constitutively activated in human prostate adenocarcinoma and correlates with disease progression. *Neoplasia* 2004, 6:390–400
36. Shukla S, MacLennan GT, Marengo SR, Resnick MI, Gupta S: Constitutive activation of P I3 K-Akt and NF- κ B during prostate cancer progression in autochthonous transgenic mouse model. *Prostate* 2005, 64:224–239
37. Phin S, Moore MW, Cotter PD: Genomic rearrangements of PTEN in prostate cancer. *Front Oncol* 2013, 3:240
38. Ittmann M, Huang J, Radaelli E, Martin P, Signoretti S, Sullivan R, Simons BW, Ward JM, Robinson BD, Chu GC, Loda M, Thomas G, Borowsky A, Cardiff RD: Animal models of human prostate cancer: the consensus report of the New York meeting of the Mouse Models of Human Cancers Consortium Prostate Pathology Committee. *Cancer Res* 2013, 73:2718–2736
39. Kramer G, Steiner GE, Handisurya A, Stix U, Haitel A, Knerer B, Gessl A, Lee C, Marberger M: Increased expression of lymphocyte-derived cytokines in benign hyperplastic prostate tissue, identification of the producing cell types, and effect of differentially expressed cytokines on stromal cell proliferation. *Prostate* 2002, 52:43–58
40. Steiner GE, Stix U, Handisurya A, Willheim M, Haitel A, Reithmayr F, Paikl D, Ecker RC, Hrachowitz K, Kramer G, Lee C, Marberger M: Cytokine expression pattern in benign prostatic hyperplasia infiltrating T cells and impact of lymphocytic infiltration on cytokine mRNA profile in prostatic tissue. *Lab Invest* 2003, 83:1131–1146
41. Robert G, Descazeaud A, Nicolaiew N, Terry S, Sirab N, Vacherot F, Maille P, Allory Y, de la Taille A: Inflammation in benign prostatic hyperplasia: a 282 patients' immunohistochemical analysis. *Prostate* 2009, 69:1774–1780
42. Gandaglia G, Briganti A, Gontero P, Mondaini N, Novara G, Salonia A, Sciarra A, Montorsi F: The role of chronic prostatic inflammation in the pathogenesis and progression of benign prostatic hyperplasia (BPH). *BJU Int* 2013, 112:432–441
43. True LD, Berger RE, Rothman I, Ross SO, Krieger JN: Prostate histopathology and the chronic prostatitis/chronic pelvic pain syndrome: a prospective biopsy study. *J Urol* 1999, 162:2014–2018
44. Gabrilovich DI, Ostrand-Rosenberg S, Bronte V: Coordinated regulation of myeloid cells by tumours. *Nat Rev Immunol* 2012, 12:253–268
45. Gabrilovich DI, Nagaraj S: Myeloid-derived suppressor cells as regulators of the immune system. *Nat Rev Immunol* 2009, 9:162–174
46. Liebig C, Ayala G, Wilks JA, Berger DH, Albo D: Perineural invasion in cancer: a review of the literature. *Cancer* 2009, 115:3379–3391
47. Katz B, Srougi M, Dall'Oglio M, Nesrallah AJ, Sant'anna AC, Pontes J Jr, Antunes AA, Reis ST, Viana N, Sanudo A, Camaralopes LH, Leite KR: Perineural invasion detection in prostate biopsy is related to recurrence-free survival in patients submitted to radical prostatectomy. *Urol Oncol* 2013, 31:175–179
48. Elharram M, Margel D, Finelli A, Trachtenberg J, Evans A, van der Kwast TH, Sweet JM, Fleshner N: Perineural invasion on prostate biopsy does not predict adverse pathological outcome. *Can J Urol* 2012, 19:6567–6572
49. Bosland MC, Prinsen MK, Dirksen TJ, Spit BJ: Characterization of adenocarcinomas of the dorsolateral prostate induced in Wistar rats by N-methyl-N-nitrosourea, 7,12-dimethylbenz(a)anthracene, and 3,2'-dimethyl-4-aminobiphenyl, following sequential treatment with cyproterone acetate and testosterone propionate. *Cancer Res* 1990, 50:700–709
50. Garabedian EM, Humphrey PA, Gordon JI: A transgenic mouse model of metastatic prostate cancer originating from neuroendocrine cells. *Proc Natl Acad Sci U S A* 1998, 95:15382–15387

51. Matzuk MM, Brown CW, Kumar TR: Transgenics in endocrinology. Totowa, NJ, Humana Press, 2001
52. Kelavkar UP, Parwani AV, Shappell SB, Martin WD: Conditional expression of human 15-lipoxygenase-1 in mouse prostate induces prostatic intraepithelial neoplasia: the FLiMP mouse model. *Neoplasia* 2006, 8:510–522
53. Martin P, Liu YN, Pierce R, Abou-Kheir W, Casey O, Seng V, Camacho D, Simpson RM, Kelly K: Prostate epithelial *Pten*/TP53 loss leads to transformation of multipotential progenitors and epithelial to mesenchymal transition. *Am J Pathol* 2011, 179:422–435
54. Borowsky AD, Dingley KH, Ubick E, Turteltaub KW, Cardiff RD, Devere-White R: Inflammation and atrophy precede prostatic neoplasia in a PhIP-induced rat model. *Neoplasia* 2006, 8:708–715
55. Li G, Wang H, Liu AB, Cheung C, Reuhl KR, Bosland MC, Yang CS: Dietary carcinogen 2-amino-1-methyl-6-phenylimidazo [4,5-b]pyridine-induced prostate carcinogenesis in CYP1A-humanized mice. *Cancer Prev Res (Phila)* 2012, 5:963–972
56. Huang H, Cheville JC, Pan Y, Roche PC, Schmidt LJ, Tindall DJ: PTEN induces chemosensitivity in PTEN-mutated prostate cancer cells by suppression of Bcl-2 expression. *J Biol Chem* 2001, 276:38830–38836
57. Majumder PK, Febbo PG, Bikoff R, Berger R, Xue Q, McMahon LM, Manola J, Brugarolas J, McDonnell TJ, Golub TR, Loda M, Lane HA, Sellers WR: mTOR inhibition reverses Akt-dependent prostate intraepithelial neoplasia through regulation of apoptotic and HIF-1-dependent pathways. *Nat Med* 2004, 10:594–601
58. Wang W, Bergh A, Damber JE: Morphological transition of proliferative inflammatory atrophy to high-grade intraepithelial neoplasia and cancer in human prostate. *Prostate* 2009, 69:1378–1386
59. Woenckhaus J, Fenic I: Proliferative inflammatory atrophy: a background lesion of prostate cancer? *Andrologia* 2008, 40:134–137
60. Terracciano D, Bruzzese D, Ferro M, Autorino R, di Lorenzo G, Buonerba C, Mariano A, Macchia V, Altieri V, di Carlo A: Soluble interleukin-6 receptor to interleukin-6 (sIL6R/IL-6) ratio in serum as a predictor of high Gleason sum at radical prostatectomy. *Oncol Lett* 2011, 2:861–864
61. Kwon EM, Salinas CA, Kolb S, Fu R, Feng Z, Stanford JL, Ostrander EA: Genetic polymorphisms in inflammation pathway genes and prostate cancer risk. *Cancer Epidemiol Biomarkers Prev* 2011, 20:923–933
62. Wegiel B, Bjartell A, Culig Z, Persson JL: Interleukin-6 activates PI3K/Akt pathway and regulates cyclin A1 to promote prostate cancer cell survival. *Int J Cancer* 2008, 122:1521–1529
63. Nguyen DP, Li J, Yadav SS, Tewari AK: Recent insights into NF-kappaB signalling pathways and the link between inflammation and prostate cancer. *BJU Int* 2014, 114:168–176